Anisotropic x ray magnetic linear dichroism

Its importance for the analysis of soft x ray spectra of magnetic oxides

G. van der Laan[1,a] and E. Arenholz[2]

[1] Diamond Light Source, Didcot, Oxfordshire OX11 0DE, UK
[2] Advanced Light Source, Lawrence Berkeley National Laboratory, Berkeley, CA

Abstract. Using spectroscopic information for x ray magnetometry and magnetic microscopy requires detailed theoretical understanding of spectral shape and magnitude of dichroism signals. We have shown unambiguously that—contrary to common belief—spectral shape and magnitude of x ray magnetic linear dichroism (XMLD) are not only determined by the relative orientation of magnetic moments and x ray polarization, but also their orientations relative to the crystallographic axes must be taken into account for accurate interpretation of XMLD data.

1 Introduction

To be able to engineer magnetic nanostructures comprised of multiple layers with very different magnetic properties for device applications in information storage technology requires a precise determination of the spin structure in heteromagnetic nanostructures. Soft x ray magnetic dichroism spectroscopies play an ever increasing role in improving our understanding of complex magnetic nanostructures as these techniques provide elemental and chemical site-specific magnetic information with high sensitivity and tunable probing depth. X ray spectromicroscopy techniques such as photoemission electron microscopy (PEEM) add spatial resolution down to a few nm. Using spectroscopic information for magnetometry and magnetic microscopy, i.e., to determine the alignment of magnetic moments relative to the crystal axes and to image domains, requires detailed knowledge and theoretical understanding of the spectral shape and magnitude of dichroism signals as well as their dependence on the relative orientation of polarization, external field, and crystallographic axes.

X ray magnetic linear dichroism (XMLD) was first predicted in 1985 [1] and observed experimentally the year after [2]. Sum rules relate the integrated intensities of the L_2 and L_3 XMLD to expectation values of charge quadrupole moment and anisotropic spin-orbit interaction [3]. Measurements and theoretical description of the anisotropic x ray magnetic linear dichroism (AXMLD) were recently obtained at the $L_{2,3}$ edges of the $3d$ transition metal oxides $NiFe_2O_4$, NiO [4], Fe_3O_4 [5], and $CoFe_2O_4$ [6] and rare earth $M_{4,5}$ edges of the ferromagnetic semiconductor EuO [7]. These results showed that—contrary to common belief—spectral shape and magnitude of the XMLD is not only determined by the relative orientation of magnetic moments and x ray polarization but that their orientations relative to the crystallographic axes has to be taken into account. Consequently, conclusions based on the interpretation of XMLD spectra without accounting for its anisotropy have to be reconsidered. In particular, previous conclusions for NiO [8–10] require a reinterpretation of the experimental data using these recent findings [4]. The XMLD angular dependence reflects the symmetry of the crystal field and is well reproduced using atomic multiplet theory [11]. The observed anisotropy in the XMLD is a general phenomenon expected in any magnetic system.

[a] e-mail: g.vanderlaan@dl.ac.uk

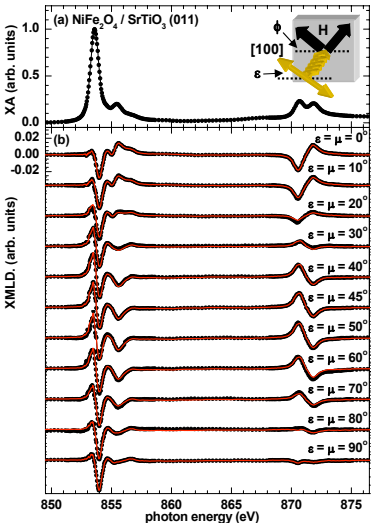

Fig. 1. (Color online) Angular dependence of the Ni $L_{2,3}$ XMLD in $NiFe_2O4/SrTiO_3(011)$. Inset: experimental geometry of field **H** (black arrows) and linear polarization **E** (yellow arrows) at angle ε to the [100] axis (dashed line). Top: X ray absorption (XA) spectrum. Bottom: XMLD spectra. Symbols indicate the experimental data and (red) lines give the results of the modeled angular dependence.

2 Ni^{2+} XMLD

In $NiFe_2O_4$ films the Ni^{2+} moments are coupled ferromagnetically and can be aligned in any in-plane direction by a external magnetic field of ∼0.5 T. X ray absorption (XA) measurements in arbitrary geometry were performed using the eight-pole resistive electromagnet [12] on beam line 4.0.2 at the Advance Light Source (ALS) with 100% linearly polarized x rays. The Ni $L_{2,3}$ XA is shown in Fig. 1(a).

The angular dependence of the XMLD signal across the Ni $L_{2,3}$ edges was obtained by rotating the orientation of x ray polarization **E** and external magnetic field **H** relative to the crystalline axes, c.f., inset to Fig. 1(a), where **E** makes an angle ε relative to the [100] crystal axis. The XMLD is the difference between XA spectra with **H** at angles μ and $\mu + 90°$ to the [100] direction, i.e., $I_{\rm xmld}(\varepsilon,\mu) = I_{\rm xa}(\varepsilon,\mu) - I_{\rm xa}(\varepsilon,\mu+90°)$, i.e., we measured the XMLD with **H**, and hence the Ni moments, parallel and perpendicular to **E** and varied the orientation of **E** relative to the crystal lattice. The XMLD angular dependence of $NiFe_2O_4/SrTiO_3(011)$ is displayed in Fig. 1(b) for $\varepsilon = \mu$ between 0° and 90°. A strong anisotropy of the XMLD signal is observed. The Ni L_2 XMLD signal reverses its sign for $\varepsilon = 0°$ and 45° and disappears almost completely for $\varepsilon = 90°$. This demonstrates that the spectral shape of the XMLD signal depends strongly on the orientations of **E** and **H** relative to the crystalline axes. Expressions for the angular dependence of the XMLD are governed by symmetry conditions [5]. For the geometry with $\mu = \varepsilon$ the XMLD signals for the (001) and (011) planes in cubic lattice are

$$I_{\rm xmld}^{(001)}(\varepsilon) = \frac{1}{2}\left[I_0 + I_{45} + (I_0 - I_{45})\cos 4\varepsilon\right],$$
$$I_{\rm xmld}^{(011)}(\varepsilon) = I_0 - \frac{1}{8}\left(5 - 2\cos 2\varepsilon - 3\cos 4\varepsilon\right)(I_0 - I_{45}),$$

where the "fundamental spectra", I_0 and I_{45}, are defined as $I_{\rm xmld}(\varepsilon = \mu = 0°)$ and $I_{\rm xmld}(\varepsilon = \mu = 45°)$, respectively. The correct description of the angular dependence in cubic crystal field requires both I_0 and I_{45} [5].

Figure 1(b) shows the excellent agreement between experimental data and modeled angular dependence. Further confirmation comes from atomic multiplet calculations for the electric-dipole transitions Ni^{2+} $3d^8 \rightarrow 2p^5 3d^9$ in octahedral crystal field. Figure 2 shows the remarkable

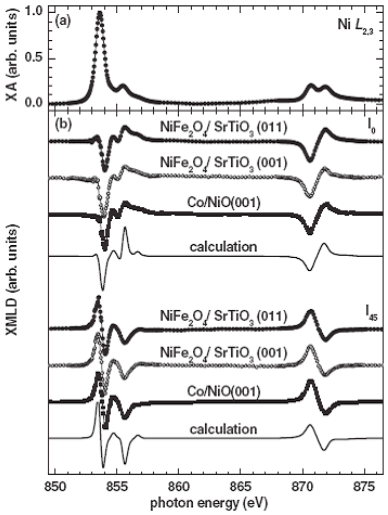

Fig. 2. Top: Measured Ni $L_{2,3}$ XA spectrum for $NiFe_2O_4/SrTiO_3$. Bottom: Comparison of the experimentally obtained fundamental XMLD spectra I_0 and I_{45} for $NiFe_2O_4$ and NiO (dots) and atomic multiplet calculations for Ni^{2+} in cubic symmetry (lines).

agreement between the calculated and experimental spectra for I_0 and I_{45}. All measured features in the spectra are reproduced by the calculation, although the feature at 855.5 eV appears overestimated.

Comparison between $NiFe_2O_4$ and NiO in Fig. 2 shows that the fundamental spectra exhibit similar spectral shapes for the ferromagnet and antiferromagnet. This is extremely useful since the fundamental spectra can be measured more easily in a ferro- or ferrimagnet and the results can then be transferred to an antiferromagnet where the moments are not so easily rearranged.

It is essential to take into account the crystal axes orientation for a correct interpretation of the XMLD for magnetometry and microscopy applications. Applying our method to revisit the exchange coupled Co/NiO(001) interface we observe, contrary to previous experimental reports [13], perpendicular coupling between Ni and Co moments, as has been predicted by some of the theoretical models [14,15], and we observe the formation of an antiferromagnetic domain wall parallel to the (001) plane upon magnetization reversal in the Co layer [4].

3 Magnetic and charge anisotropy

The XMLD shows a large angular dependence for the high-spin half-filled Fe d^5 configuration in Fe_3O_4 with cubic symmetry [5], despite the fact that both charge quadrupole moment and anisotropic spin-orbit interaction vanish in this case. The same is observed for tetrahedral Mn d^5 in the ferromagnetic semiconductor (Ga,Mn)As [16]. This suggests that the angular dependence can not be ascribed to the magnetocrystalline anisotropy [17]. Instead, the angular dependence is a property of the cubic wave functions for the $3d$ valence states with respect to the spin quantization axis. The AXMLD can be used to estimate the size of the crystal field splitting and allows determining the spin quantization axis with respect to the crystalline axes. The magnetocrystalline anisotropy manifests itself only in the integrated intensities of the L_3 and L_2 XMLD signals [3,18,19], which are small compared to the huge angular peak variations.

The electric-dipole selection rules restrict the set of final states that can be reached from the ground state. This gives different transition probabilities from the exchange-split core levels to the crystal-field-split empty $3d$ states. Multiplet calculations show that the angular dependence of the XMLD signal disappears when the crystal field splitting goes to zero. Therefore, anisotropic XMLD is a property of the cubic wavefunctions for the d states with respect to the spin quantization axis, and not the anisotropic spin-orbit interaction.

In cubic crystal field symmetry the XMLD is a linear combination of the two fundamental spectra, I_0 and I_{45}, each exhibiting a distinctly different spectral shape, but with the same shape when rotating either **E** or **H** [5]. In contrast, in tetragonal distorted crystal field the XMLD is a linear combination of four fundamental spectra, with different shapes for rotation of either **E** or **H** [6]. The difference in the fundamental spectra for linear dichroism (i.e., rotation of **E**) and magnetic dichroism (i.e., rotation of **H**) allows us to assess the influence of the charge anisotropy due to non-cubic distortion, as has been shown for CoO [6].

In cubic systems the orientation of the spin axis with respect to the crystallographic axes can be studied with PEEM by rotating **E** [20]. With caution, also non-cubic systems can be studied by rotating **E**, as this is the preferred method for PEEM. In the case of strongly distorted cubic symmetry the analysis of the linear dichroism is more complicated due to the charge anisotropy. On the other hand, the magnetic dichroism remains largely unaffected for such a symmetry distortion [6].

4 Europium oxide

Rare earths systems also show AXMLD, although much weaker. The AXMLD at the Eu^{2+} $M_{4,5}$ edges of EuO(001) is very well described by the same model used for the cubic transition metal oxides [7]. Multiplet calculations for Eu $4f^7$ show that the magnitude of the AXMLD varies linearly with the strength of the effective crystalline electric field (CEF). The measured AXMLD evidences a considerable energy splitting of the $4f$ orbitals. The observed charge anisotropy present in each of the non-degenerate $4f$ states demonstrates the feasibility of pinning the $4f$ states by the local environment and tuning by external conditions, chemical doping, or strain for purposes in device applications.

The Advanced Light Source is supported by the Director, Office of Science, Office of Basic Energy Sciences, of the U.S. Department of Energy under Contract No. DE-AC02-05CH11231.

References

1. B.T. Thole, G. van der Laan, and G.A. Sawatzky, Phys. Rev. Lett. **55**, (1985) 2086
2. G. van der Laan, B.T. Thole, G.A. Sawatzky, J.B. Goedkoop, J.C. Fuggle, J.M. Esteva, R.C. Karnatak, J.P. Remeika, and H.A. Dabkowska, Phys. Rev. B **34**, (1986) 6529
3. G. van der Laan, Phys. Rev. Lett. **82**, (1999) 640
4. E. Arenholz, G. van der Laan, R.V. Chopdekar, and Y. Suzuki, Phys. Rev. Lett. **98**, (2007) 197201
5. E. Arenholz, G. van der Laan, R.V. Chopdekar, and Y. Suzuki, Phys. Rev. B **74**, (2006) 094407
6. G. van der Laan, E. Arenholz, R.V. Chopdekar, and Y. Suzuki, Phys. Rev. B **77**, (2008) 064407
7. G. van der Laan, E. Arenholz, A. Schmehl, and D.G. Schlom, Phys. Rev. Lett. **100**, (2008) 067403
8. D. Alders, L.H. Tjeng, F.C. Voogt, T. Hibma, G.A. Sawatzky, C.T. Chen, J. Vogel, M. Sacchi, and Iacobucci, Phys. Rev. B **57** (1998) 11623
9. J. Stöhr, A. Scholl, T.J. Regan, S. Anders, J. Lüning, M.R. Scheinfein, H.A. Padmore, and R.L. White, Phys. Rev. Lett. **83** (1999)1862
10. H. Ohldag, A. Scholl, F. Nolting, S. Anders, F.U. Hillebrecht, and J. Stöhr, Phys. Rev. Lett. **86** (2001) 2878
11. G. van der Laan and B.T. Thole, Phys. Rev. B **43**, (1991) 13401
12. E. Arenholz and S.O. Prestemon, Rev. Sci. Instrum. **76** (2005) 083908
13. A. Scholl, M. Liberati, E. Arenholz, H. Ohldag, and J. Stöhr, Phys. Rev. Lett. **92** (2004) 247201
14. N.C. Koon, Phys. Rev. Lett. **78**, (1997) 4865
15. T.C. Schulthess and W.H. Butler, Phys. Rev. Lett. **81**, (1998) 4516
16. A.A. Freeman, K.W. Edmonds, G. van der Laan, N.R.S. Farley, T.K. Johal, E. Arenholz, R.P. Campion, C.T. Foxon, and B.L. Gallagher, Phys. Rev. B **73**, (2006) 233303
17. J. Kunes and P.M. Oppener, Phys. Rev. B **67** (2003) 024431
18. G. van der Laan, Phys. Rev. B **55**, (1997) 8086
19. G. van der Laan, Phys. Rev. B **57**, (1998) 112
20. S. Czekaj, F. Nolting, L.J. Heyderman, P.W. Willmott, and G. van der Laan, Phys. Rev. B **73**, (2006) 020401